



Parametrization of irregularity of urban morphologies for designing better pedestrian wind environment in high-density cities – A wind tunnel study

Yueyang He^{a,*}, Zhixin Liu^b, Edward Ng^{a,b,c}

^a Institute of Future Cities, The Chinese University of Hong Kong, Hong Kong, China

^b School of Architecture, The Chinese University of Hong Kong, Hong Kong, China

^c Institute of Environment, Energy and Sustainability, The Chinese University of Hong Kong, Hong Kong, China

ARTICLE INFO

Keywords:

Urban morphometric study
Morphological parameter
Open-space
Urban ventilation
GIS mapping
Urban design

ABSTRACT

Breezeways are crucial for horizontal urban ventilation. However, their morphologies, which are highly irregular, still lack investigation. This study aims to gain a categorical understanding of how irregular breezeway morphologies affect pedestrian-level wind performance in high-density cities. Firstly, we extracted breezeway areas and centerlines by adopting different definitions of breezeways: Method 1 defining all near-ground open-spaces (i.e., roads, other non-building areas, and low-rise-building areas) as breezeways; Method 2 defining roads as breezeways. Secondly, multiple morphological parameters were developed to describe irregularity (i.e., fragmentation, angularity, and sinuosity) and permeability of 19 typical urban sites in Hong Kong. Thirdly, linear regression analysis was conducted to correlate the parameters with wind tunnel data. The results show that in a dense built environment, urban ventilation relies on morphologies of all near-ground open-spaces rather than only roads. The regression analysis reveals a negative correlation between pedestrian-level wind performance and urban irregularity, where fragmentation has the largest impact due to the increase of building wall surfaces and viscous friction. The regression analysis reveals a positive correlation between pedestrian-level wind performance and urban permeability, where the newly-defined parameter (i.e., open-space width), which incorporates fragmentation into calculation, achieves higher coefficient of determination than the widely-used parameter (i.e., open-space coverage ratio). The newly-developed regression model, which considers both urban permeability and irregularity, predicts wind speed with a simple mathematical manipulation and a comparable accuracy to models in previous studies. More importantly, it provides applicable spatial information of urban irregularity for design of open-spaces and improvement of urban ventilation.

1. Introduction

1.1. Background

Urban dwellers, especially those living in high-density cities, are vulnerable to health threats caused by the growing environmental issues, such as global climate change [1], urban heat island effects [2], and pollutant/disease transmissions [3]. Designing cities with better urban ventilation could help to mitigate these threats and improve the living environment. As many cities increasingly densify, the need for a better understanding of the urban wind environment becomes paramount.

Hong Kong, located in the sub-tropical climate zone, has one of the highest living densities in the world. Due to the fast urbanization over

the past 50 decades, the mean wind speed in the built-up areas has decreased dramatically [4]. It motivates the local communities to optimize urban designs for a better pedestrian-level wind environment [5]. To this end, in 2006, the government bureaus issued the “Technical Circular (TC06-01) on Air Ventilation Assessments (AVA)” [6], which requires developers to adopt wind tunnel and Computational Fluid Dynamics (CFD) simulations to assess their designs. Later, the Planning Department incorporated the new guidelines on air ventilation into the “Urban Design Guidelines (Chapter 11), Hong Kong Planning Standards and Guidelines” [7]. They provided qualitative guidance on building and breezeway designs in the district and neighborhood scales. In 2011, the Building Department issued the “Sustainable Building Design Guidelines (APP-152)” [8], which provided a few quantitative design parameters and guidance in the building and street scales. These wind-related urban design standards and guidelines were produced with

* Corresponding author.

E-mail address: yueyanghe@cuhk.edu.hk (Y. He).

<https://doi.org/10.1016/j.buildenv.2022.109692>

Received 26 August 2022; Received in revised form 6 October 2022; Accepted 8 October 2022

Available online 17 October 2022

0360-1323/© 2022 Elsevier Ltd. All rights reserved.

Nomenclature			
<i>Parameters</i>		$l_{OS,i}$	centerline length of open-space segment i
C_{OS}	open-space coverage ratio	$l_{RD,i}$	centerline length of road segment i
C_{RD}	road coverage ratio	o_x	x-coordinate of center point of open-space cell
D_{OS}	open-space centerline density	o_y	y-coordinate of center point of open-space cell
D_{RD}	road centerline density	P_i	calculated value of parameter at urban site i
R_{OS}	open-space intersection rotation angle	P_i^*	normalized value of parameter at urban site i
R_{RD}	road intersection rotation angle	P_{min}	minimum value of parameter at all urban sites
S_{OS}	open-space segment sinuosity	P_{max}	maximum value of parameter at all urban sites
S_{RD}	road segment sinuosity	$p\text{-Value}$	significant level
W_{OS}	open-space width	R^2	coefficient of determination
W_{RD}	road width	$RMSE$	root-mean-square error
<i>Other symbols</i>		U_i	urban wind speed (2 m) at test point i
A_T	total area of target urban site	$U_{\infty,WT}$	upwind wind speed (500 m) applied in wind tunnel
A_i	area of breezeway segment i	$U_{\infty,LiDAR}$	upwind wind speed (500 m) observed by LiDAR
$A_{OS,i}$	area of open-space segment i	VR	spatially-averaged wind velocity ratio (2 m)
$A_{RD,i}$	area of road segment i	VR_i	wind velocity ratio (2 m) at test point i
b_x	x-coordinate of center point of building source	z_0	roughness length
b_y	y-coordinate of center point of building source	z_d	zero-plane displacement length
$d(o,b)$	Euclidean distance of open-space and building	α_i	rotation angle of breezeway intersection i
d_i	two-endpoint distance of breezeway segment i	$\alpha_{regular,i}$	minimum regular angle fitting α_i
$d_{OS,i}$	two-endpoint distance of open-space segment i	$\alpha_{OS,i}$	rotation angle of open-space intersection i
$d_{RD,i}$	two-endpoint distance of road segment i	$\alpha_{RD,i}$	rotation angle of road intersection i
l_i	centerline length of breezeway segment i	τ_f	form drag
		τ_s	skin drag

the studies on a portion of urban morphological characteristics in Hong Kong and other high-density cities.

1.2. Morphometric studies on urban aerodynamics

As one of the roughest and most complicated surface properties, urban morphologies generate form drag (τ_f) induced by the pressure on roughness elements and skin drag (τ_s) induced by the friction between fluid and element (e.g., building) surfaces. They influence the aerodynamic conductance for momentum transport [9], scales and intensity of turbulence [10], and magnitude and shape of wind speed profile [11]. Relevant urban morphometric studies have been conducted with two main focuses:

- 1) algorithms to correlate theoretic aerodynamic parameters with urban morphologies or terrain types, as well as gain knowledge of the aerodynamic characteristics of cities; and
- 2) empirical models using practical morphological parameters to predict urban wind distribution, as well as provide guidance for urban ventilation designs.

With the first focus, studies have established different methods to estimate surface roughness, and determine the values of roughness length (z_0) and zero-plane displacement length (z_d) through parametrization of surface morphological characteristics. These characteristics mainly included mean building height [12–14], plan area ratio [15–17], and frontal area index [18–20]. Based on the morphologies of 11 urban sites, Grimmond and Oke [10] tested different methods and recommended the optimal ones for determining the aerodynamic parameters in urban areas. Based on over 60 field experiments, Wieringa [21,22] revised the Davenport roughness classification, which suggested proper z_0 for different homogeneous terrain types. These studies developed the theoretical understanding of the relation between urban roughness and wind.

With the second focus, studies have adopted more practical morphological parameters to predict urban permeability and wind

performance. Among these studies, Matzarakis and Mayer [23] used the effective heights derived from mean heights of buildings, vegetation, and other open-spaces to develop the wind map in Munich. Kubota et al. [24] established empirical models between plan area ratio and pedestrian-level wind performance with 22 residential neighborhoods in Japanese cities. Gál and Unger [25] calculated the porosity of the urban canopy layer together with z_0 and z_d , and drew the wind map in Szeged. Wong et al. [26] and Ng et al. [27] used frontal area index of buildings to predict the regional air paths in Hong Kong. Based on plan area ratio, frontal area index and area-weighted mean building height, Suder and Szymanowski [28] estimated the wind distribution in Wrocław. Based on frontal area index, Yuan et al. [29] and Xie et al. [30] predicted the regional air paths in Wuhan, and Hsieh and Huang [31] generated the wind maps in Tainan. Tschritzis and Nikolopoulou [32] associated façade area ratio and other morphological parameters of building heights with pedestrian-level wind comfort in London. Palusci et al. [33] established the correlation between morphological parameters, such as plan area ratio, building height, volume density and façade area density, and urban ventilation in Rome. These studies made quantitative and visual evaluations of wind environment for urban designs.

1.3. Research gaps and objectives

As reviewed in the aforementioned literatures, studies have well addressed the impacts of urban roughness and permeability on wind performance, but there is still a lack of exploration and parametrization of the influence of irregularity of urban morphologies. This may be because the irregularity is difficult to be described by the characteristics of roughness elements (e.g., mean building height, plan area ratio, and frontal area index). The lack of such studies, from the theoretical perspective, might lead to an underestimation of the impacts of τ_s , as the parameters of roughness elements mainly consider τ_f , while τ_s can actually be dominant in porous bodies (e.g., fragmented urban areas) as revealed by the studies of turbulent flow (e.g., flow in water pipes [34] and street canyons [35]). From the practical perspective, due to the little progress in relevant research, there is still insufficient quantitative

parameters to guide designs in irregular urban areas which are commonly seen in major cities.

To fill the knowledge gap, this study aims to gain and collate a categorical understanding of how irregular urban morphologies affect pedestrian-level wind performance in high-density cities. The irregularity is described by the network patterns of breezeways. As defined by Ng [5], the urban breezeways can be formed of different elements, such as roads, other non-building areas (e.g., parks and squares), and low-rise-building areas (Fig. 1), and their morphologies are very complicated. Although a good breezeway design is beneficial to urban ventilation, comprehensively describing these morphologies is challenging. Therefore, it is essential to extend the existing understanding of urban breezeways and provide quantitative guidance to breezeway designs for better urban ventilation.

2. Methodology

This section introduces three steps to attain the research objective. Section 2.1 extracts breezeway areas and centerlines based on two different definitions of breezeways. Section 2.2 parameterizes irregular characteristics of the extracted breezeway morphologies. Section 2.3 acquires wind tunnel experimental data to correlate pedestrian-level wind performance with the parameters of irregular characteristics. 19 high-density urban sites from the wind tunnel benchmarking dataset in Hong Kong [36] are selected to calculate the parameters. As shown in Fig. 2, the target sites are scattered over the whole city and represent various typical urban morphologies. Their descriptions are listed in Table 1.

2.1. Extraction of breezeway areas and centerlines

To prepare for the calculation of parameters, we adopted two different methods to extract breezeway areas and centerlines at the target urban sites from Geographic Information System (GIS) data. Based on the definition in Fig. 1, the Method 1 defined all near-ground open-spaces (i.e., roads, other non-building areas, and low-rise-building areas) to be breezeways as it assumed that these areas are freely penetrated by wind. In this method, low-rise buildings were defined to have no more than three stories (i.e., ≤ 9 m) referring to the classification criterion related to building aerodynamics recommended by Architectural Institute of Japan (AIJ) [37] and the typical height limit of land houses controlled by Hong Kong's building ordinance [38]. Respectively, the Method 2 defined only roads to be breezeways given that they were usually considered to be the major corridors of wind in high-density urban areas. Fig. 3 presents the areas of the extracted open-spaces and roads at the target urban sites. It should be noted that the actual areas of breezeways could be overestimated by the Method 1 and underestimated by the Method 2, and the optimal method is determined by the regression analysis results in Section 3.2.

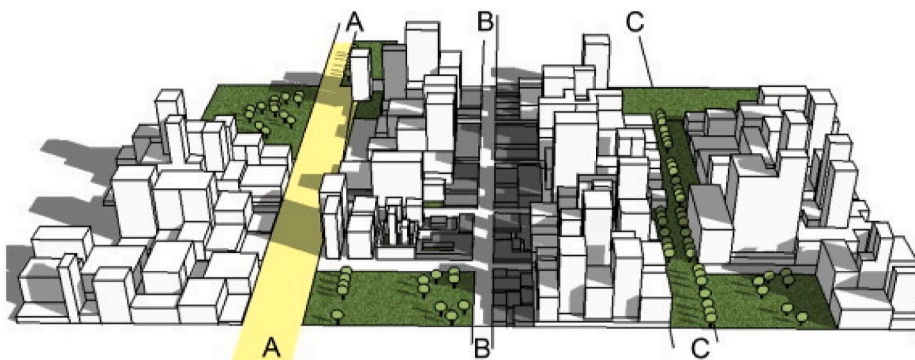


Fig. 1. Types of breezeways in high-density urban areas (A-A: roads as a breezeway; B-B: low-rise-building areas as a breezeway; and C-C: other non-building areas (e.g., parks and squares) as a breezeway), defined by Ng [5].

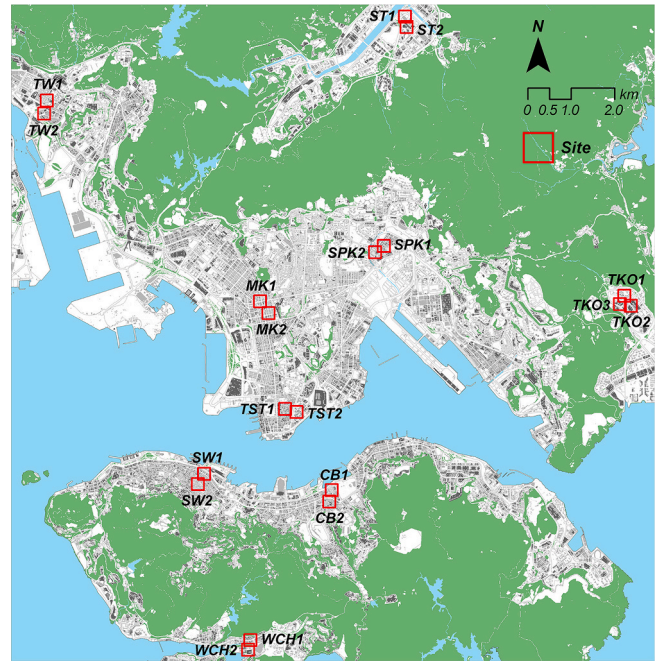


Fig. 2. Target urban sites (300 m \times 300 m) in Hong Kong for calculating breezeway morphological parameters and conducting regression analysis with pedestrian-level wind performance.

Based on the extracted breezeway areas, the Method 1 further extracted their centerlines by calculating the Euclidean distance [39] from each open-space cell in the raster to the closest building source:

$$d(o, b) = \sqrt{(o_x - b_x)^2 + (o_y - b_y)^2} \quad (1)$$

where o_x and o_y are the Cartesian coordinates of the center point of each open-space cell; and b_x and b_y are the Cartesian coordinates of the center point of the closest building source. After the calculations, each open-space cell was allocated to the zone surrounding a building source based on closest proximity. The boundaries of these surrounding zones were identified as the breezeway centerlines. To ensure a high-resolution of the centerlines, the extractions applied 0.1 m cell size in the raster. Meanwhile, the Method 2 directly adopted GIS data of road centerlines to represent breezeway centerlines. Fig. 4 shows an example to use the two methods to extract breezeway centerlines.

Table 1
Descriptions of target urban sites in Hong Kong.

ID	Description	Image	ID	Description	Image
TW1	Tsuen Wan 1 A downtown site (since 1950s) characterized by a majority of adjacent medium-rise buildings and a few high-rise buildings		TW2	Tsuen Wan 2 An industrial site (since 1950s) occupied by medium-rise to high-rise bulky buildings with linked podiums	
ST1	Sha Tin 1 A new town site (since 1970s) with scattered high-rise point-shaped buildings and central medium-rise bulky buildings		ST2	Sha Tin 2 A new town site (since 1970s) formed by high-rise point-shaped buildings with bulky-podiums or no-podiums	
MK1	Mong Kok 1 A downtown site (since pre-1950s) occupied by adjacent medium-rise to high-rise buildings		MK2	Mong Kok 2 A downtown site (since pre-1950s) occupied by adjacent medium-rise to high-rise buildings	
SPK1	San Po Kong 1 An industrial site (since 1960s) occupied by medium-rise to high-rise bulky buildings with linked podiums		SPK2	San Po Kong 2 A downtown site (since 1960s) with a mixture of adjacent medium-rise buildings and high-rise buildings on linked podiums	
TKO1	Tseung Kwan O 1 A new town site (since 1980s) with a mixture of medium-rise to high-rise slab-shaped and point-shaped buildings		TKO2	Tseung Kwan O 2 A new town site (since 1980s) characterized by bulky podiums and high-rise point-shaped buildings	
TKO3	Tseung Kwan O 3 A new town site (since 1980s) characterized by bulky podiums and high-rise point-shaped buildings		TST1	Tsim Sha Tsui 1 A downtown site (since pre-1950s) occupied by medium-rise to high-rise adjacent buildings	
TST2	Tsim Sha Tsui 2 A reclaimed downtown site (since 1980s) formed by medium-rise to high-rise bulky buildings on individual podiums		SW1	Sheung Wan 1 A downtown site (since pre-1950s) consists of adjacent high-rise buildings and a few individual high-rise buildings	
SW2	Sheung Wan 2 A downtown site (since pre-1950s) occupied by adjacent medium-rise to high-rise buildings		CB1	Causeway Bay 1 A downtown site (since pre-1950s) consists of adjacent medium-rise to high-rise buildings	
CB2	Causeway Bay 2 A downtown site (since pre-1950s) consists of adjacent medium-rise to high-rise buildings		WCH1	Wong Chuk Hang 1 An industrial site (since 1960s) formed by high-rise slab-shaped buildings and a few adjacent medium-rise buildings	
WCH2	Wong Chuk Hang 2 A new town site (since 1990s) with a mixture of a few medium-rise buildings and high-rise point-shaped buildings				

2.2. Calculation of breezeway morphological parameters

Based on the extracted breezeway areas and centerlines in Section 2.1, we established multiple parameters to describe breezeway morphologies at the target urban sites. The parameters considered two aspects of morphological characteristics, including irregularity (i.e., fragmentation, angularity, and sinuosity) and permeability. They were calculated at each target urban site by self-developed Python scripts. Diagrams of the parameters' calculation are introduced in Fig. 5, with more detailed explanations from Sections 2.2.1 to 2.2.4. It should be clarified that since most of the flow above high-density urban canopy is skimming [40] and near-ground flow behaviors are largely determined by their horizontal motions, this study only focused on two-dimensional breezeway morphological parameters; the characteristics of building

heights (i.e., distinguishing low-rise buildings from middle-rise and high-rise buildings) were considered when extracting breezeway areas and centerlines in Section 2.1.

2.2.1. Fragmentation

Fragmentation of an urban site refers to the degree of breaking up integrated building clusters or urban blocks into separated ones. It is usually indicated by parameters related to the network patterns of open-spaces or roads as they are the major elements that divide a landscape [41,42] (i.e., urban landscape). The impacts of the fragmentation on pedestrian-level wind environment have not been sufficiently studied and there were only a few relevant case studies. In the street scale, Shen et al. [43] developed opening ratio to represent the fragmentation in six actual urban streets. They revealed a stronger channeling flow in the

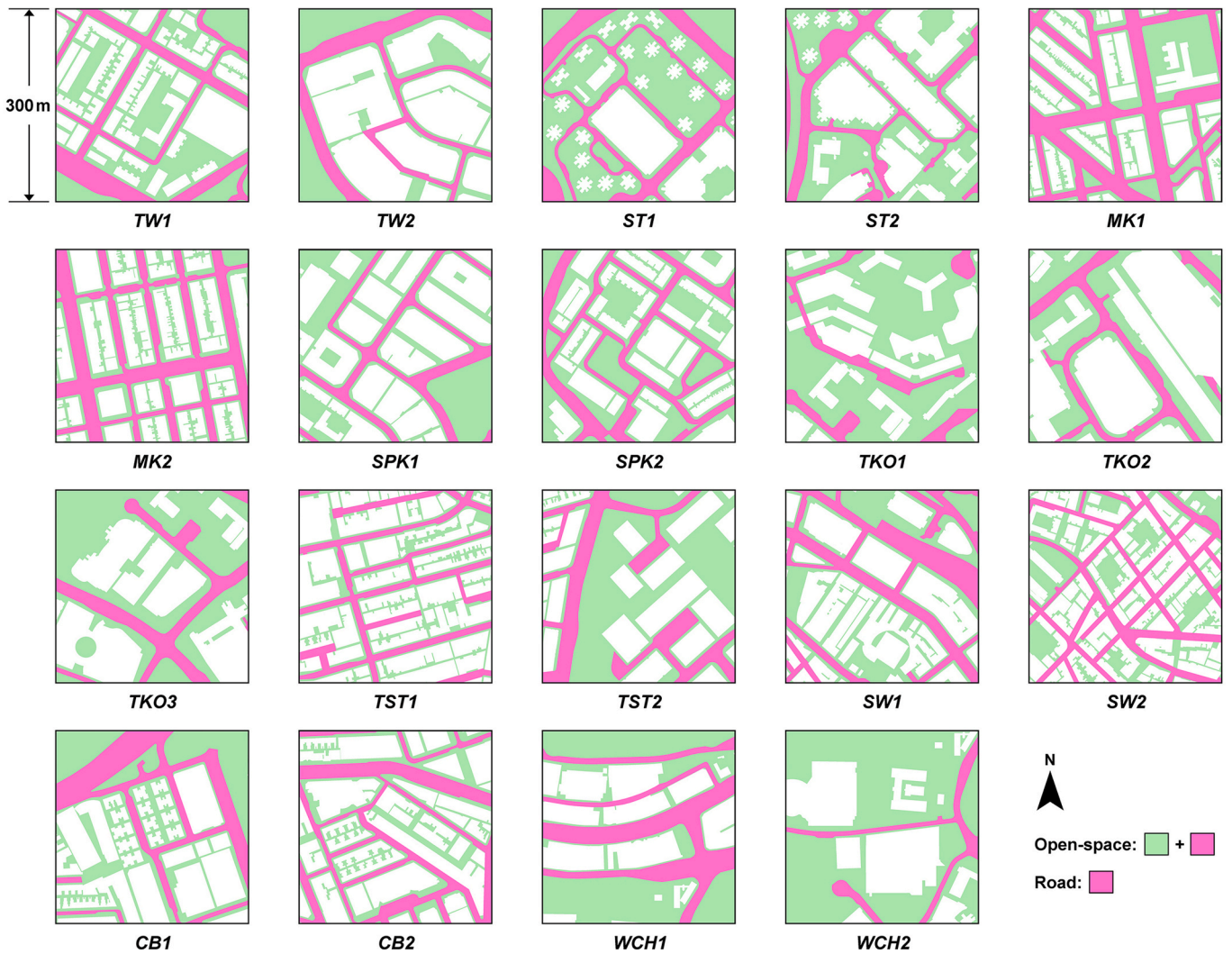


Fig. 3. Breezeway areas at target urban sites extracted by two methods: the Method 1 (i.e., all near-ground open-spaces as indicated by the green and purple areas) and the Method 2 (i.e., roads as indicated by the purple areas). (For interpretation of the references to colour in this figure legend, the reader is referred to the Web version of this article.)

street with fewer lateral openings and a higher symmetry. In the neighborhood scale, He et al. [44] used road density to describe the fragmentation in three high-density urban areas. Their results correlated higher urban wind speed with a coarser road network. Given the limited existing research, the correlation between fragmentation and pedestrian-level wind environment needs a further study.

Based on a neighborhood scale, this study quantified fragmentation of the target urban sites by two parameters, i.e., open-space centerline density (D_{OS}) and road centerline density (D_{RD}):

$$D_{OS} = \frac{\sum_{i=1}^n l_{OS-i}}{A_T} \quad (2)$$

$$D_{RD} = \frac{\sum_{i=1}^m l_{RD-i}}{A_T} \quad (3)$$

where $l_{OS,i}$ and $l_{RD,i}$ are the centerline lengths of the open-space and road segment i , respectively; n and m are the number of the open-space and road centerline segments, respectively; and A_T is the total area of the target urban sites. This study defined the integrated morphology of urban areas as one of the benchmark characteristics of regularity, and a more fragmented morphology (i.e., higher D_{OS} and D_{RD}) is more irregular.

2.2.2. Angularity

Angularity of an urban site represents the degree of transforming orthogonal open-space or road intersections into angular (i.e., non-orthogonal) ones. Compared with the widely-studied orthogonal intersections, much less studies discussed the non-orthogonal ones. Case studies have categorized different flow behaviors in some generic non-orthogonal intersections, such as three-way, four-way, and circular intersections [45–47]. Besides, a comprehensive parametric study [48] has been conducted on the impacts of rotation angles (i.e., from 0° to 45°) of four-way intersections on pedestrian-level wind performance. The study revealed very different flow regime and velocity between orthogonal and angular intersections. Except these studies, no relevant study has parametrized actual urban morphologies where various irregular intersections exist.

This study quantified angularity of the target urban sites by establishing two parameters, i.e., open-space intersection rotation angle (R_{OS}) and road intersection rotation angle (R_{RD}):

$$R_{OS} = \frac{\sum_{i=1}^j (\alpha_{OS-i} - \alpha_{regular-i})}{n} \quad (4)$$

$$R_{RD} = \frac{\sum_{i=1}^k (\alpha_{RD-i} - \alpha_{regular-i})}{m} \quad (5)$$

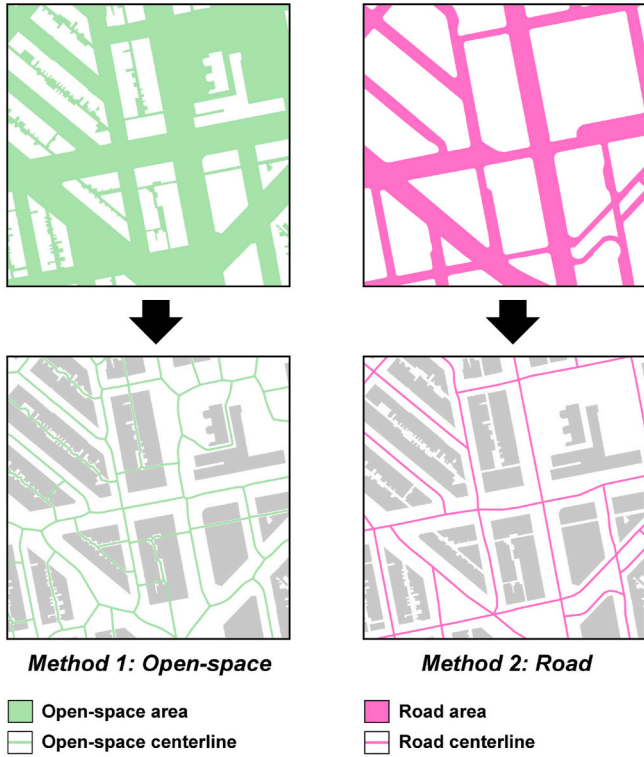


Fig. 4. Diagrams of using two methods to extract breezeway centerlines at an urban site (e.g., MK1).

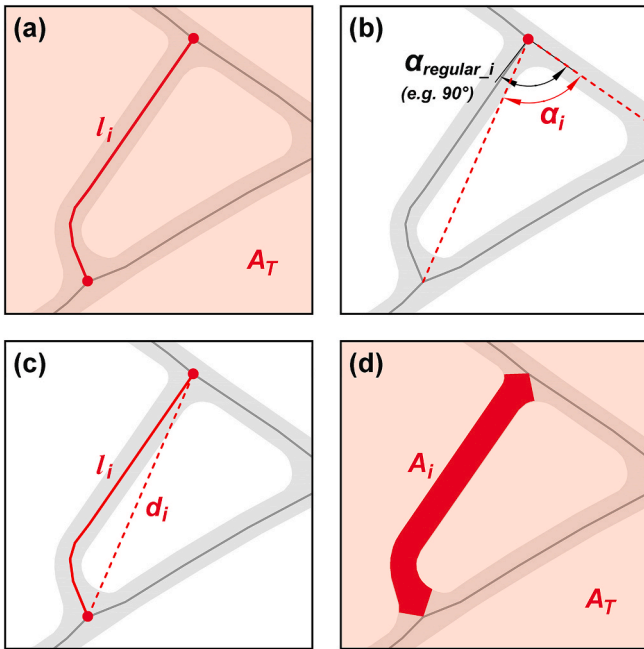


Fig. 5. Diagrams of the calculation of breezeway morphological parameters: (a) open-space/road centerline density (D_{OS}/D_{RD}); (b) open-space/road intersection rotation angle (R_{OS}/R_{RD}); (c) open-space/road segment sinuosity (S_{OS}/S_{RD}); and (d) open-space/road coverage ratio (C_{OS}/C_{RD}).

where α_{OS_i} and α_{RD_i} are the rotation angles of the open-space and road intersection i , respectively; j and k are the number of the open-space and road intersections, respectively; and $\alpha_{regular_i}$ is the minimum regular angle that fit α_{OS_i} and α_{RD_i} . Specifically, $\alpha_{regular_i}$ is defined to be 0° , 90° , 180° , 270° , and 360° when α_{OS_i} and α_{RD_i} are within the ranges of $<45^\circ$,

$45\text{--}135^\circ$, $135\text{--}225^\circ$, $225\text{--}315^\circ$, and $\geq 315^\circ$, respectively. This study defined the orthogonal morphology of breezeway intersections as one of the benchmark characteristics of regularity, and a more angular morphology (i.e., higher R_{OS} and R_{RD}) is more irregular.

2.2.3. Sinuosity

Sinuosity of an urban site refers to the degree of transforming straight open-space or road segments into sinuous (i.e., non-straight) ones. Sinuosity is known to be highly correlated with flow behaviors (e.g., flow in rivers [49,50]), and relevant parameters have been adopted to describe its impacts on urban flow. For example, Adolphe [51] calculated the sinuosity of urban streets in order to identify the difference between street orientations and prevailing wind direction in three cities. Based on wind tunnel experiments, Li et al. [52] introduced the non-linear coefficient to distinguish the sinuosity in asymmetry-square and diagonal-square road networks. They found a lower wind speed in the diagonal-square road network where the sinuosity was higher.

In this study, sinuosity of the target urban sites was quantified by two parameters, i.e., open-space segment sinuosity (S_{OS}) and road segment sinuosity (S_{RD}):

$$S_{OS} = \frac{\sum_{i=1}^n l_{OS_i} (l_{OS_i} / d_{OS_i})}{\sum_{i=1}^n l_{OS_i}} \quad (6)$$

$$S_{RD} = \frac{\sum_{i=1}^m l_{RD_i} (l_{RD_i} / d_{RD_i})}{\sum_{i=1}^m l_{RD_i}} \quad (7)$$

where d_{OS_i} and d_{RD_i} are the straight-line distances between the two endpoints of the open-space and road segment i , respectively. This study defined the straight morphology of breezeway segments as one of the benchmark characteristics of regularity, and a more sinuous morphology (i.e., higher S_{OS} and S_{RD}) is more irregular.

2.2.4. Permeability

Permeability of an urban site refers to its capability for flows to pass through it. Compared with the irregularity (i.e., fragmentation, angularity, and sinuosity), the permeability has been applied more widely in previous studies where, as mentioned in Section 1.2, the plan area ratio and frontal area index were commonly used to indicate the horizontal and vertical permeability, respectively. To be consistent with the previous studies, this study used two similar parameters to represent the horizontal permeability induced by open-spaces and roads, i.e., open-space coverage ratio (C_{OS}) and road coverage ratio (C_{RD}):

$$C_{OS} = \frac{\sum_{i=1}^n A_{OS_i}}{A_T} \quad (8)$$

$$C_{RD} = \frac{\sum_{i=1}^m A_{RD_i}}{A_T} \quad (9)$$

where A_{OS_i} and A_{RD_i} are the areas of the open-space and road segment i , respectively. More than these two parameters, we defined another two new parameters by incorporating the irregularity (i.e., fragmentation) into the calculation of permeability, i.e., open-space width (W_{OS}) and road width (W_{RD}):

$$W_{OS} = \frac{C_{OS}}{D_{OS}} = \frac{\sum_{i=1}^n A_{OS_i}}{\sum_{i=1}^n l_{OS_i}} \quad (10)$$

$$W_{RD} = \frac{C_{RD}}{D_{RD}} = \frac{\sum_{i=1}^m A_{RD_i}}{\sum_{i=1}^m l_{RD_i}} \quad (11)$$

The effect of incorporating the irregularity in the calculation of permeability is evaluated by comparing these two sets of permeability parameters in Section 3.

2.3. Acquisition of pedestrian-level wind data

To correlate the parameters established in Section 2.2 with wind performance, this study acquires the pedestrian-level wind data at the target urban sites from wind tunnel experiments [53,54]. The experiments were set according to the AVA technical circular [6]. Reduced-scale (1: 400) urban models (Appendix A) were tested under the city's long-term-averaged upwind wind conditions in 16 cardinal directions [4]. Multi-point thermal anemometers were evenly distributed at each target urban site to measure the pedestrian-level (i.e., 2 m above the ground in full-scale) wind speed. Based on the multi-point wind speed, the spatially-averaged wind velocity ratio (VR) at each urban site was calculated:

$$VR = \frac{1}{n} \sum_{i=1}^n VR_i = \frac{1}{n} \sum_{i=1}^n \frac{U_i}{U_{\infty,WT}} \quad (12)$$

where VR_i refers to the 16-wind-direction-averaged wind velocity ratio at the test point i ; U_i refers to the 16-wind-direction-averaged pedestrian-level wind speed at the test point i ; $U_{\infty,WT}$ refers to the upwind wind speed at an upper height (i.e., 500 m above the ground in full-scale) applied in the wind tunnel experiments; and n refers to the number of test points at the target urban site. Fig. 6 plots the distribution of VR_i and VR at each target urban site.

3. Results of categorical and regression analysis

This section analyzes the results obtained by the three steps in Section 2. The categorical analysis of breezeway morphological parameters at different target urban sites is presented in Section 3.1, while the regression analysis between these parameters and pedestrian-level wind performance is presented in Section 3.2.

3.1. Results of categorical morphology analysis

To facilitate the categorical analysis of the breezeway morphological parameters at the target urban sites, we normalized the calculated values of each parameter in Section 2.2 by the following equation:

$$P_i^* = \frac{P_i - P_{min}}{P_{max} - P_{min}} \quad (13)$$

where P_i refers to the value of a study parameter calculated at the urban site i , and P_{max} and P_{min} refer to the maximum and minimum values of this parameter among all the target urban sites, respectively. After the normalization, all parameters ranged from 0 to 1 (i.e., $D_{OS/RD}^*$, $R_{OS/RD}^*$, and $S_{OS/RD}^*$ indicate the increasing irregularity from 0 to 1; $C_{OS/RD}^*$ and $W_{OS/RD}^*$ indicate the increasing permeability from 0 to 1).

The normalized parameters of all target urban sites are plotted in

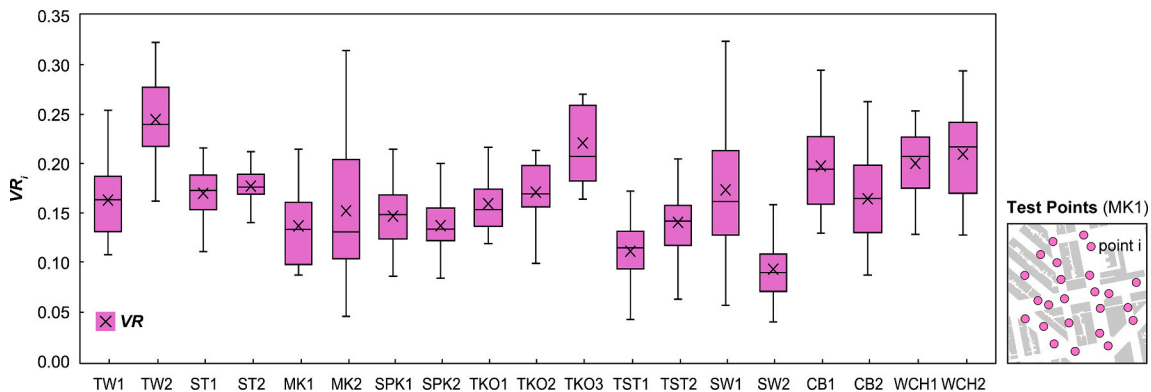


Fig. 6. Fluctuation of wind velocity ratio (VR_i) across test points and their spatially-averaged value (VR) at each target urban site from wind tunnel experiments [53, 54] (e.g., VR_i at 24 test points of MK1 fluctuating from 0.09 to 0.22 and their VR reaching 0.14).

Fig. 7. Overall, the open-space-based method (i.e., the Method 1) and road-based method (i.e., the Method 2) obtain different calculation results of both the irregularity and permeability. The difference is significant especially when the site morphologies are complicated.

Fragmentation: With the Method 1, the least fragmented morphologies ($D_{OS}^* \leq 0.1$) are found at the new town and industrial sites (e.g., TKO2, TKO3, WCH1, and TW2) which consist of bulky podium structures and integrated open-spaces, while the most fragmented sites ($D_{OS}^* \geq 0.6$) are found at the downtowns (e.g., TW1, TST1, SW2, and MK2) where buildings are small and open-spaces are narrow. Similar calculation results are obtained by the Method 2 except the relatively large difference found at some downtown sites (e.g., CB2 and SW1).

Angularity: Based on the Method 1, the downtown sites with orthogonal patterns (e.g., MK2, TST1, and TW1) are the least angular ($R_{OS}^* \leq 0.4$) and their downtown counterparts with non-orthogonal patterns are confirmed to be more angular (e.g., SW2, CB2, and MK1). The most angular sites ($R_{OS}^* \geq 0.8$) are located at the new towns (e.g., ST1, TKO1, and TKO2) where the open-spaces are complicated by the sparsely-distributed and non-uniformly-shaped buildings. Compared with the Method 1, the Method 2 indicates less angular morphologies in some new town sites where the difference between R_{OS}^* and R_{RD}^* can be over 0.5 (e.g., TKO1, TKO3, and ST1).

Sinuosity: Different from the fragmentation and angularity, the sinuosity is hardly identified by the site types. The Method 1 indicates the least sinuous morphologies ($S_{OS}^* \leq 0.1$) in all site types: the downtown (e.g., MK2 and CB1), new town (e.g., ST1), and industrial sites (e.g., SPK1 and WCH1). Meanwhile, the most sinuous sites ($S_{OS}^* \geq 0.7$) are also found in both the downtowns (e.g., MK1 and SW2) and new towns (e.g., TKO1 and TKO2). Their relatively high sinuosity is attributed to the presence of some long and non-straight buildings, which form adjacent open-spaces into L-shapes or U-shapes. In comparison, the Method 2 indicates different and even opposite results at some sites, e.g., ST1 ($S_{OS}^* = 0.1$; $S_{RD}^* = 1.0$), MK1 ($S_{OS}^* = 0.8$; $S_{RD}^* = 0$), and SW2 ($S_{OS}^* = 0.7$; $S_{RD}^* = 0.1$).

Permeability: Both parameters (C_{OS}^* and W_{OS}^*) based on the Method 1 indicate higher permeability at most of the new town and industrial sites, and lower permeability at most of the downtown sites. Differently, with the Method 2 (C_{RD}^* and W_{RD}^*), some downtown and new town sites have the highest and lowest permeability respectively, and the permeability varies largely at the industrial sites.

To understand how the irregularity (i.e., fragmentation) affects the calculation of the permeability, the four normalized parameters of the permeability are compared in Fig. 8. With the Method 1, by incorporating the fragmentation into C_{OS}^* , W_{OS}^* indicates significantly higher permeability at some sites with more integrated building and open-space morphologies (e.g., TW2 and TKO2), while shows lower permeability at some sites with more fragmented or scattered morphologies (e.g., MK1 and ST1). With the Method 2, however, the two parameters (C_{RD}^* and

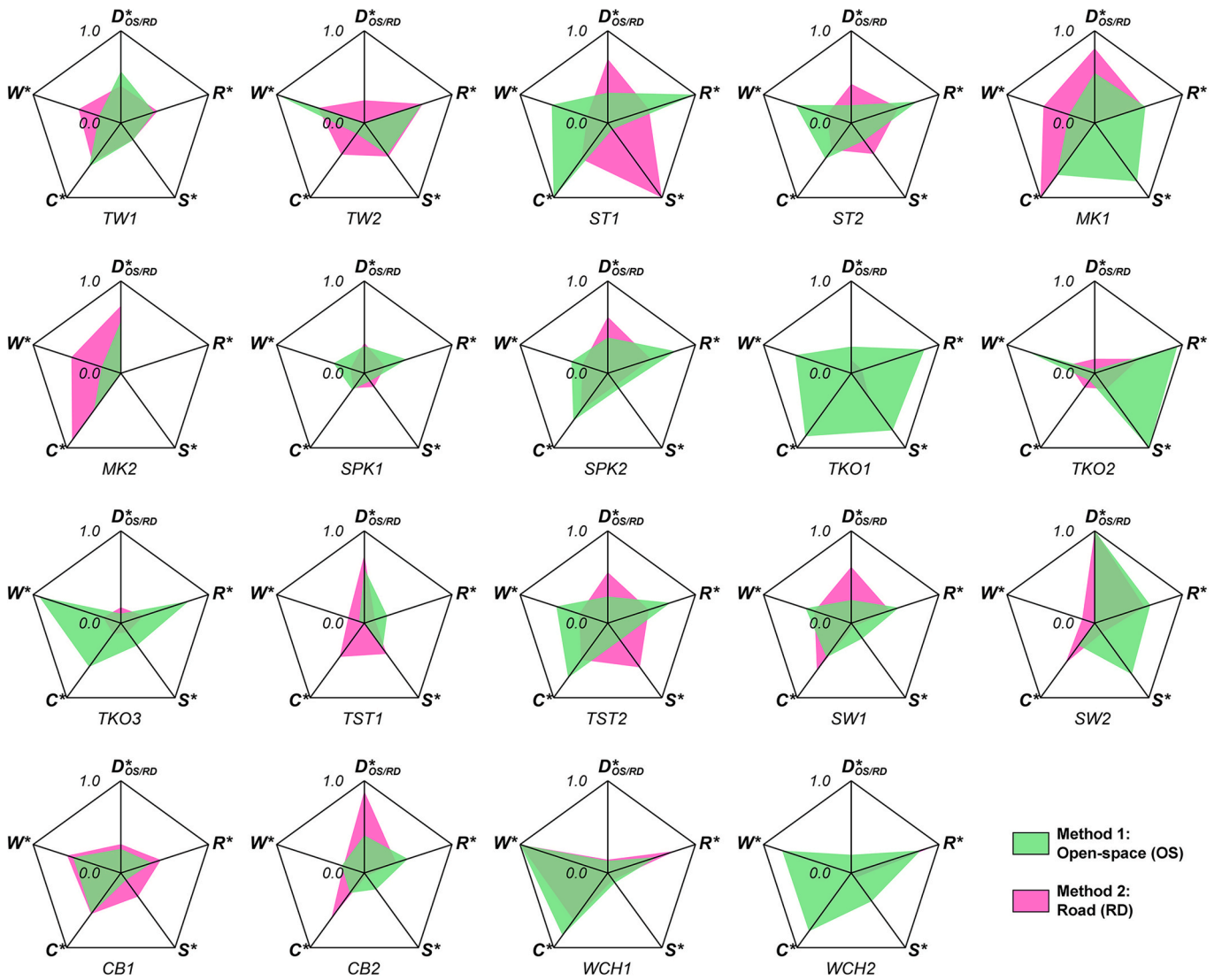


Fig. 7. Values of normalized breezeway morphological parameters at target urban sites calculated by two methods (note: $D_{OS/RD}^*$, $R_{OS/RD}^*$ and $S_{OS/RD}^*$ indicate the increasing irregularity from 0 to 1; $C_{OS/RD}^*$ and $W_{OS/RD}^*$ indicate the increasing permeability from 0 to 1).

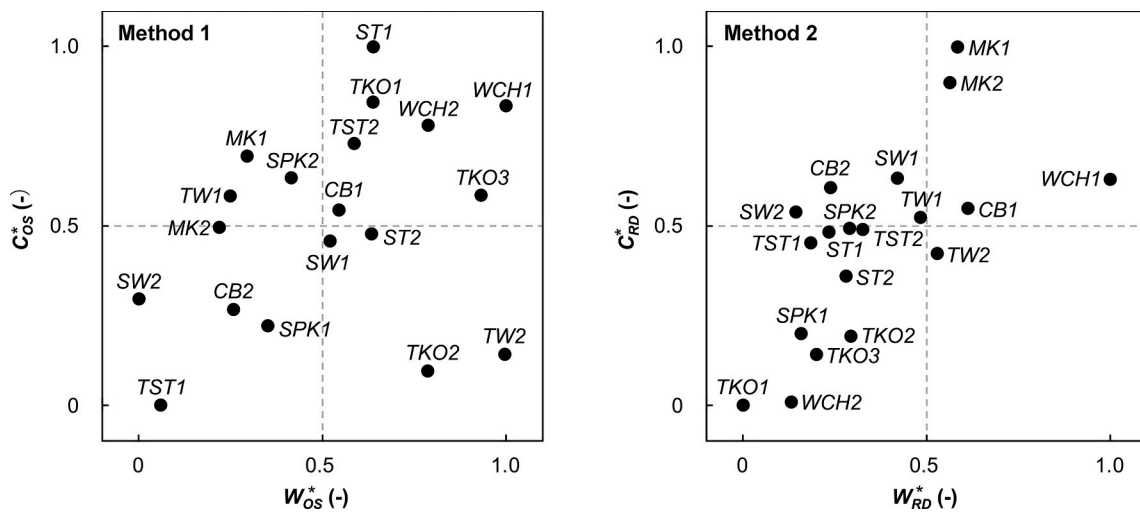


Fig. 8. Normalized open-space/road coverage ratio (C_{OS}^* / C_{RD}^*) versus open-space/road width (W_{OS}^* / W_{RD}^*) at target urban sites.

W_{RD}^a) are relatively consistent probably due to the small variations of road widths across the city.

3.2. Results of regression analysis

To explore the impacts of the breezeway morphological parameters in Section 2.2 on pedestrian-level wind performance, firstly, we established simple linear regression between each parameter and the VR data obtained in Section 2.3. Secondly, we further established a multiple linear regression model to explain VR using a stepwise method.

3.2.1. Simple regression

The linear regression analysis results between VR and single breezeway morphological parameter are plotted in Fig. 9. Their correlations are indicated by the values of coefficient of determination (R^2).

Open-space versus road morphology: Overall, the results confirm that VR has a higher correlation with the open-space-based parameters than the road-based parameters. The results suggest that in a high-density urban area, pedestrian-level wind performance relies on the morphologies of all open-spaces (i.e., the Method 1) rather than only roads (i.e., the Method 2). It implies that VR can be improved more effectively when roads are properly integrated with other near-ground open-spaces. Compared with the road-based parameters, the open-

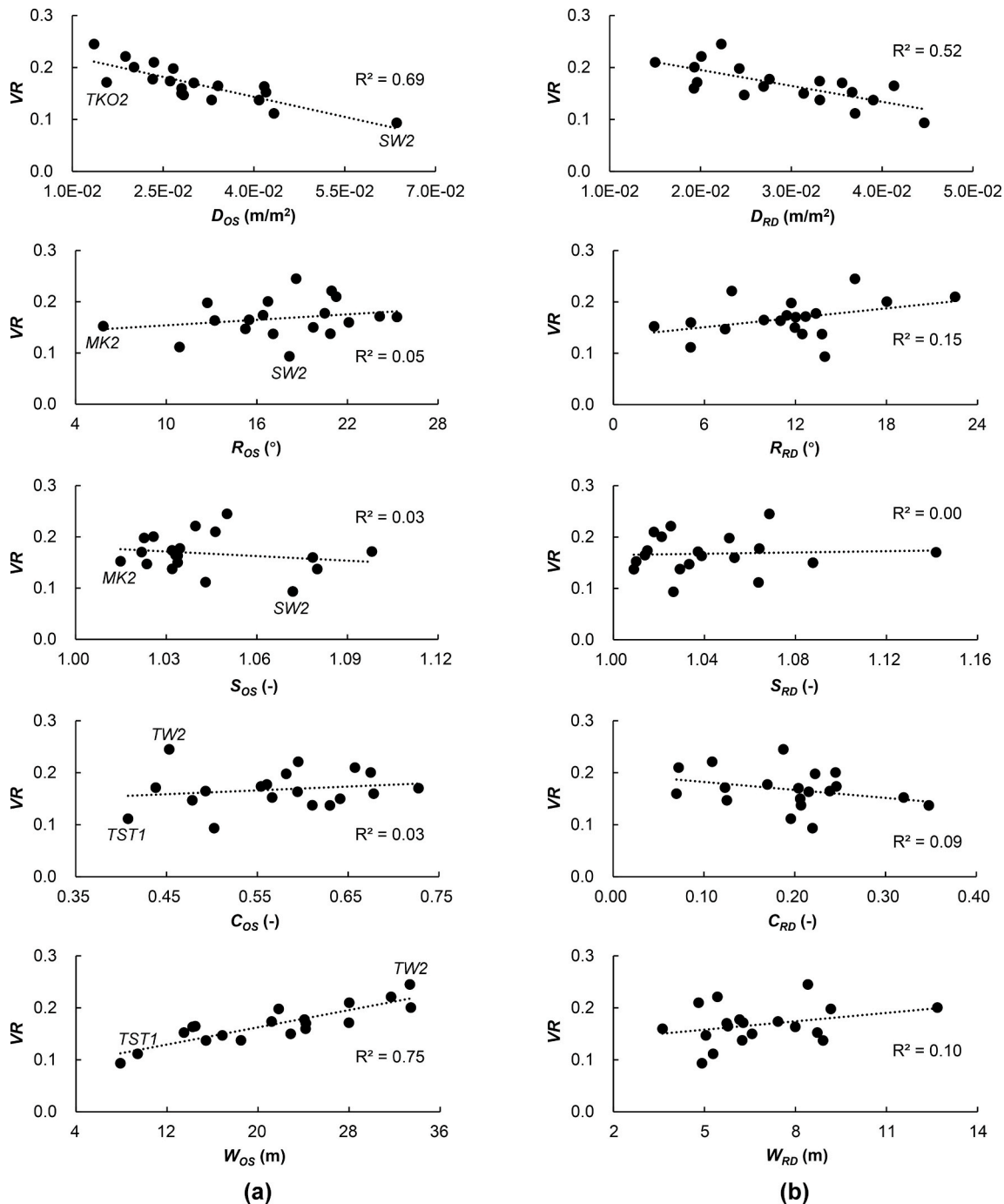


Fig. 9. Relations between ten breezeway morphological parameters and pedestrian-level wind velocity ratio (VR) obtained by (a) open-space-based method (i.e., the Method 1); and (b) road-based method (i.e., the Method 2).

space-based parameters produce more accurate regression results for VR particularly at the urban sites with lower building density (e.g., TKO1 and WCH2) where roads are only a small portion of open-spaces (Fig. 3). Given the higher R² made by the open-space parameters, we mainly focus on these parameters in the following regression analysis.

Fragmentation: The results reveal a negative correlation between VR and urban irregularity. Among the three relevant open-space-based parameters (i.e., D_{OS}, R_{OS}, and S_{OS}), D_{OS} reaches the highest R² (0.69). This tendency indicates fragmentation to be the primary irregular morphological characteristics that affects the wind performance. A main reason for this tendency is that in a compact built environment, a more fragmented urban site tends to have more building wall surfaces (e.g., SW2 versus TKO2), and generate more resistance and viscosity [55] to the horizontal flow in the urban canopy. The higher fragmentation also distributes the channelization effect [56], hence further reducing the flow velocity.

Permeability: A positive correlation is confirmed between VR and urban permeability. Between the two open-space-based parameters (i.e., C_{OS} and W_{OS}), C_{OS} shows a lower R² due to a few outliers (e.g., TW2). However, for most of the data points, the correlation between C_{OS} and VR is significant, and in line with the previous findings [24,33,57] in wind tunnel and CFD studies. Fig. 10 shows the consistency between most of the data points in this study and those obtained by Kubota et al. [24] in middle-rise and high-rise urban areas. Alternatively, W_{OS} shows a higher R² (0.75). Differently from C_{OS}, W_{OS} considers fragmentation (i.e., D_{OS}) in the calculation, and is capable to identify the different VR in narrow and wide breezeways at the target urban sites (e.g., TST1 versus TW2) even though they have a similar building/open-space coverage. The relation between flow behaviors and breezeway widths has been well understood in the street scale [40,58,59], while the new calculation method of W_{OS} provides a possible way to extend this understanding to actual urban areas with more complicated morphologies.

Angularity and sinuosity: The results in Fig. 9 show a low R² (below 0.1) for both R_{OS} and S_{OS}. However, Fig. 11 more clearly reveals the negative correlations (i.e., R² = 0.4–0.9) between VR and the two parameters by classifying the results in Fig. 9 with three ranges of W_{OS}. The results imply that angularity and sinuosity can be the secondary irregular morphological characteristics which still largely determine the wind performance when W_{OS} is fixed. This tendency can be attributed to the flow resistance enhanced by the more inhomogeneous breezeway intersections and segments at an irregular urban site (e.g., MK2 versus SW2). The tendency is also consistent with the results in previous experimental and numerical studies [60–62] which distinguished the aerodynamic effects between regular and irregular morphologies.

3.2.2. Multiple regression

The multiple linear regression analysis result between VR and the ten breezeway morphological parameters is shown in Fig. 12. Based on a stepwise method, two open-space-based parameters (i.e., W_{OS} and R_{OS}) finally enter into the regression model:

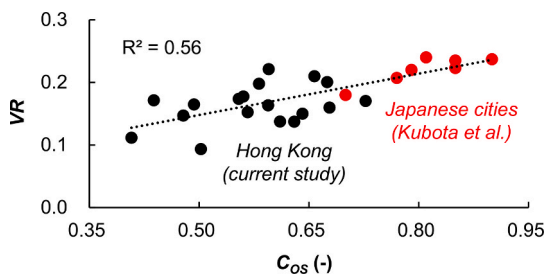


Fig. 10. Relations between C_{OS} and pedestrian-level wind velocity ratio (VR) based on most of the data points (i.e., data point at TW2 was excluded) in the current study and the data points obtained in middle-rise and high-rise urban areas by Kubota et al. [24] (where C_{OS} = 1 – plan area ratio).

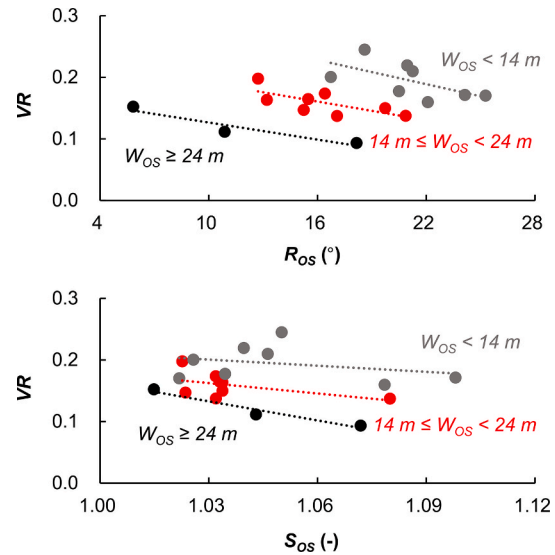


Fig. 11. Relations between two irregularity parameters (R_{OS} and S_{OS}) and pedestrian-level wind velocity ratio (VR) classified in three ranges of open-space widths: (1) W_{OS} < 14 m (R² = 0.38/0.09 for R_{OS}/S_{OS}); (2) 14 m ≤ W_{OS} < 24 m (R² = 0.50/0.25 for R_{OS}/S_{OS}); and (3) W_{OS} ≥ 24 m (R² = 0.90/0.95 for R_{OS}/S_{OS}).

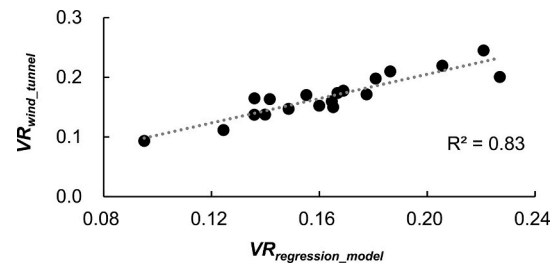


Fig. 12. The stepwise linear regression model with breezeway morphological parameters on pedestrian-level wind velocity ratio (VR) (model accuracy: RMSE = 0.015; p-Value < 0.0001).

$$VR = 0.005W_{OS} - 0.003R_{OS} + 0.105 \quad (14)$$

The accuracy of the modelling result is validated by the value of R² (0.83) and root-mean-square error (RMSE) (0.015). The result shows that using GIS data of open-space morphologies to estimate VR is more likely to be accurate than using road data. The model further implies that both urban permeability and irregularity significantly affect pedestrian-level wind performance, where a higher VR is associated with higher permeability and lower fragmentation (i.e., a higher W_{OS}), as well as lower angularity (i.e., a lower R_{OS}) of an urban site. It should be noted that D_{OS}, which shows a high R² in the simple regression analysis in Section 3.2.1, is excluded by the stepwise method in the regression model since the impact of fragmentation has been considered by W_{OS}.

4. Implementations in urban designs and discussion

This section takes Hong Kong as an example to implement the breezeway morphological parameters and multiple regression model in urban designs. Section 4.1 draws GIS maps of urban permeability and irregularity using the relevant parameters. Section 4.2 generates a pedestrian-level wind speed map using the regression model. Finally, Section 4.3 discusses the strengths and limitations of this study in terms of the parameters and the regression model.

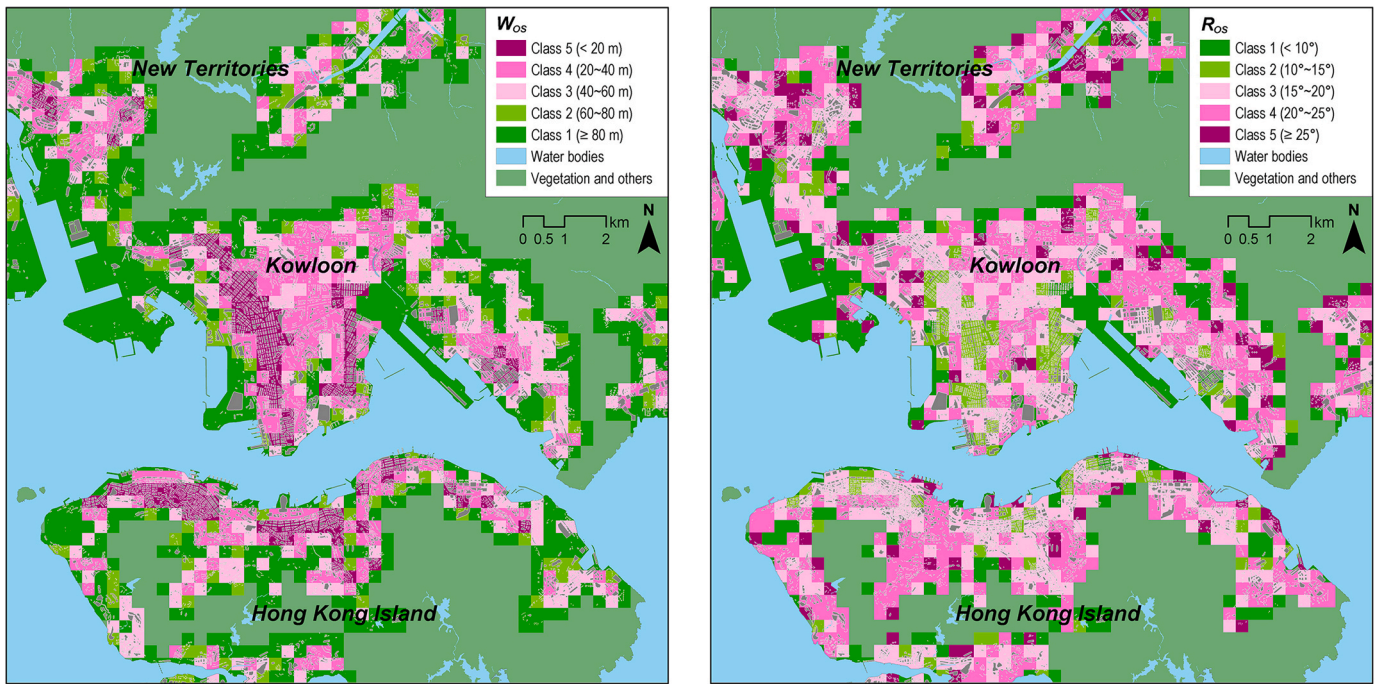


Fig. 13. GIS maps of permeability and irregularity in Hong Kong’s major urban areas based on two breezeway morphological parameters, i.e., W_{OS} and R_{OS} (note: W_{OS} is defined to be the cell width (i.e., 300 m) when D_{OS} is 0).

4.1. Implementation in classifying urban permeability and irregularity

The breezeway morphological parameters (e.g., W_{OS} and R_{OS} , which are found to have the strongest correlation with VR in Eq. (14)) can be adopted to classify the spatial distributions of urban permeability and irregularity in high-density cities. Fig. 13 shows an example of drawing GIS maps in Hong Kong’s major urban areas. To be consistent with the size of the target urban sites in the regression analysis, the maps adopted a grid resolution of 300 m.

Based on the maps of urban permeability and irregularity, urban practitioners (e.g., urban planners, designers, and architects) can easily locate the urban areas with certain ranges of permeability and/or irregularity. In the example of Hong Kong, the urban permeability map indicates several continuous urban areas with the smallest W_{OS} (i.e., Class 5) in the northern Hong Kong Island, and the western and eastern Kowloon peninsula, suggesting that the built environment in these areas is extremely dense and fragmented. A less dense built environment can be found in the New Territories since only a few of scattered neighborhoods have the smallest W_{OS} . The urban irregularity map further indicates higher R_{OS} in Hong Kong Island (e.g., Classes 3–4 in Central and Western District) than Kowloon peninsula (e.g., Class 2 in a large part of Yau Tsim Mong District), suggesting that the least permeable areas (i.e., W_{OS} of Class 5) in Hong Kong Island are more irregular and may have poor urban ventilation.

4.2. Implementation in predicting pedestrian-level wind speed

Furthermore, the established multiple regression model (Eq. (14)) may be applied to predict pedestrian-level wind speed in high-density cities. An example in Hong Kong’s major urban areas is shown in Fig. 14. To convert the modeling VR into wind speed, the prediction integrated the upper-air wind data observed by ground-based wind Light Detection and Ranging (LiDAR) [63,64]. Hourly-averaged wind speed ($U_{\infty, LiDAR}$) at 500 m above the ground (Appendix B) in summers of 2020 and 2021 at three regions of the city (i.e., Hong Kong Island (Yam Pak Building, Sai Wan), Kowloon (King’s Park Meteorological Station, Tsim Sha Tsui), and the New Territories (Air Quality Research Supersite, Sai

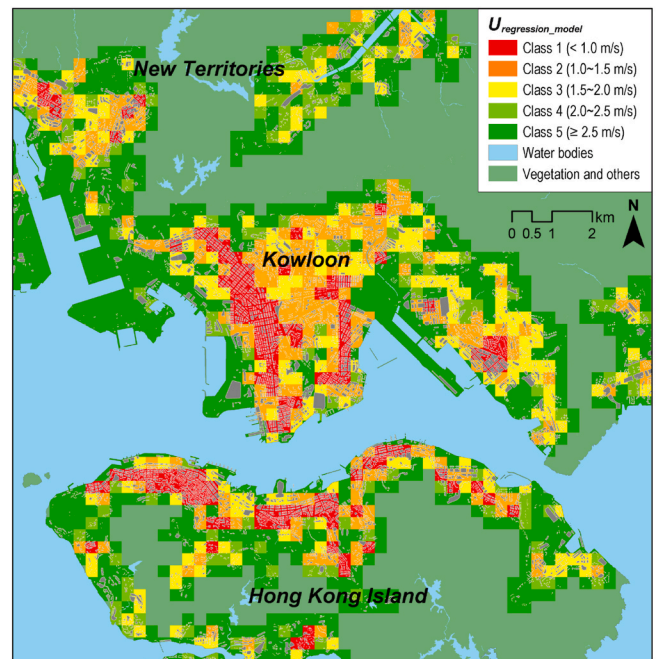


Fig. 14. GIS map of pedestrian-level wind speed (U) based on the developed multiple regression model ($R^2 = 0.83$) and the LiDAR data.

Kung)) were used to calculate the pedestrian-level wind speed:

$$U = VR \bullet U_{\infty, LiDAR} \tag{15}$$

The wind speed map provides visual information of classification of urban areas based on their wind performance. Policy makers can take into account this information in their short-term to long-term planning strategies to renew the urban areas where the flow is weak or stagnant. Particularly, since the wind speed map in this study integrated the LiDAR data, it could be a reliable tool to evaluate the influence of wind

speed on outdoor air pollutants and thermal comfort. In the example of Hong Kong, the wind speed map indicates continuous areas of wind speed <1.0 m/s (i.e., Class 1) in Hong Kong Island and Kowloon. These areas may be vulnerable to the overheating as they can hardly achieve thermal comfort in summers [65] in accordance with the criterion established in Hong Kong, and therefore may need planning actions.

4.3. Discussion on strengths and limitations

4.3.1. Newly-defined breezeway morphological parameters

Strengths: The breezeway morphological parameters in this study provides spatial information of urban irregularity, which may deepen the understanding of urban morphologies obtained by other parameters in the previous studies shown in Table 2. These parameters might be applicable to urban practitioners. They could formulate more targeted strategies, such as widening open-spaces [66] (e.g., building setbacks at podium level) in areas with high D_{OS} , and optimizing the linkages of different types of open-spaces [67] (e.g., roads, void desks, pocket parks, etc.) in areas with high R_{OS} , to design open-spaces and improve pedestrian-level wind environment in different urban areas. More importantly, the newly-defined parameter, W_{OS} , which includes fragmentation during the calculation, provides complementary information with the widely-used parameter, C_{OS} (or plan area ratio). Fig. 15 shows an example of using both W_{OS} and C_{OS} to estimate the least permeable urban areas in Hong Kong, where the attention should be mainly paid to the overlapping areas of the two parameters (i.e., $W_{OS} < 20\text{ m}$ and $C_{OS} < 0.6$) as they have the narrowest breezeways and largest building coverage.

Limitations: The breezeway morphological parameters in this study may be difficult to apply in very low-density areas or areas fully

Table 2

Morphological parameters, data grid resolutions, and validation methods adopted in previous studies reviewed in Section 1.2.

Ref.	Year	Morphological parameter	Data grid resolution	Validation method
Matzarakis and Mayer [23]	1992	Effective height	250 m	N.A.
Kubota et al. [24]	2008	Plan area ratio, gross floor area ratio	270 m	Wind tunnel
Gál and Unger [25]	2009	Plan area ratio, frontal area index, volumetrically-averaged building height, porosity of urban canopy layer	50 m	N.A.
Wong et al. [26]	2010	Frontal area index	100 m	Fieldwork
Ng et al. [27]	2011	Frontal area index, plan area ratio	50–300 m	Wind tunnel
Suder and Szymanowski [28]	2014	Plan area ratio, frontal area index, area-weighted mean building height	>50 m	N.A.
Yuan et al. [29]	2014	Frontal area index	100 m	Wind tunnel
Hsieh and Huang [31]	2016	Frontal area index	50/100 m	CFD
Tsichritzis and Nikolopoulou [32]	2019	Façade area ratio, mean building height, maximum building height	500 m	CFD
Xie et al. [30]	2020	Frontal area index	100 m	CFD
Palusci et al. [33]	2022	Plan area ratio, mean building height, root mean square of building height, median of building height, area-weighted mean building height, volume density, façade area density	250/300 m	CFD

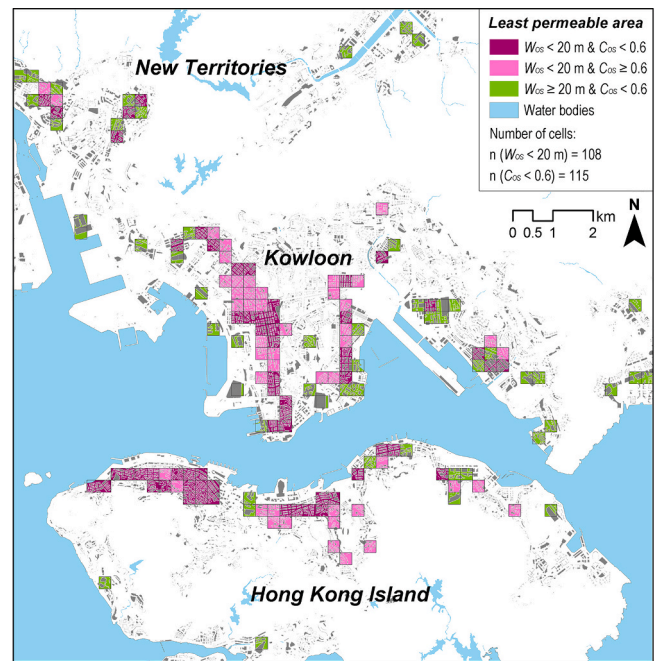


Fig. 15. GIS map of urban areas with the lowest permeability: $W_{OS} (<20\text{ m})$ versus $C_{OS} (<0.6)$.

occupied by an extremely bulky building as the extraction of breezeway centerlines in these areas could be imprecise. Besides, the parameters only consider two-dimensional urban morphologies. However, since the correlations between the breezeway morphological parameters and pedestrian-level wind performance discussed in this study show the feasibility to further explore the influence of urban irregularity on wind environment quantitatively, three-dimensional urban and topographic morphologies are expected to be taken into account in the future studies.

4.3.2. Newly-established regression model

Strengths: The newly-established regression model provides a simple mathematical manipulation to predict the pedestrian-level wind speed. Moreover, the prediction accuracy ($R^2 = 0.83$) is competitive with those ($R^2 = 0.7$ to 0.9) in previous studies reviewed in Section 1.2.

Limitations: The accuracy of the new model is only validated in the neighborhood scale (i.e., 300 m). Although the mapping resolution used in this study is consistent with the ones typically used in previous studies (Table 2), and known to optimally explain the impacts of the high-density urban morphologies [68], further validation would be necessary if the current model is applied with a finer mapping resolution or for urban designs with more street-scale details.

5. Conclusion

This study parametrically explores the influence of irregular characteristics of high-density urban morphologies on pedestrian-level wind environment in Hong Kong. Firstly, breezeway areas and centerlines of 19 target sites were extracted by adopting different definitions of breezeways: the Method 1 – defining all near-ground open-spaces (i.e., roads, other non-building areas, and low-rise-building areas) as breezeways; and the Method 2 – defining roads as breezeways. Secondly, multiple parameters were established to calculate irregularity (i.e., fragmentation, angularity, and sinuosity) and permeability based on the extracted breezeway morphologies. Thirdly, linear regression was developed between the parameters and wind tunnel data. As an implementation of the regression analysis results, GIS maps were drawn to indicate the spatial distributions of urban irregularity and pedestrian-level wind speed in Hong Kong’s major urban areas. Major findings

are listed as follows:

- The morphological analysis categorizes the characteristics of irregularity and permeability at different urban sites. The sites in downtowns tend to have higher degree of fragmentation, and lower angularity and permeability, while the sites in new towns and industrial areas show the opposite trends.
- The regression analysis confirms that in high-density urban areas, pedestrian-level wind performance relies on the morphologies of all near-ground open-spaces rather than only roads. It means that using GIS data of non-building and low-rise-building areas to estimate wind speed is more likely to achieve an accurate result than using road data.
- The regression results reveal a negative correlation between pedestrian-level wind performance and urban irregularity. Fragmentation (D_{OS}) has the primary impact, and the impacts of angularity (R_{OS}) and sinuosity (S_{OS}) are secondary. This tendency is attributed to the increase of building wall surfaces and geometric inhomogeneity in more irregular urban areas where more resistance and viscosity are generated to horizontal flow.
- The regression results also point out a positive correlation between pedestrian-level wind performance and urban permeability. Compared with the widely-used parameter (C_{OS}), which is calculated based on site coverage, the newly-defined parameter (W_{OS}), which includes fragmentation (D_{OS}) during the calculation, achieves a stronger correlation. This result is probably because the new-defined parameter is capable to identify different aerodynamic effects between narrow and wide breezeways in actual urban morphologies.

The outcomes of this study may be further implemented in urban designs to improve the wind environment in high-density areas:

- The breezeway morphological parameters provide compensatory information to the government’s “Urban Design Guidelines (Chapter 11), Hong Kong Planning Standards and Guidelines” [7] and “Sustainable Building Design Guidelines (APP-152)” [8]. These current guidelines on air ventilation are mainly applicable to regular street network patterns, while an update may be needed to make both

qualitative and quantitative recommendations to orient and link the irregular roads and other pedestrian open-spaces.

- The multiple regression model may be a starting point to develop a decision-making tool for urban ventilation designs although more further studies are necessary. It could predict wind speed at the pedestrian level with a simple mathematical manipulation and a competitive accuracy. The model could also complement the government’s Air Ventilation Assessments (AVA) methods [6] and visualize wind speed data in larger spatial scales.

The categorical understanding of urban irregularity introduces an effective method to analyze irregular urban morphologies. It is particularly valuable for high-density cities suffering from weak wind conditions. A quantitative understanding of urban irregularity may develop more targeted urban design strategies for better wind environment in these cities.

CRedit authorship contribution statement

Yueyang He: Software, Methodology, Formal analysis, Writing – original draft, Writing – review & editing. **Zhixin Liu:** Software, Methodology, Writing – review & editing. **Edward Ng:** Supervision, Methodology, Funding acquisition, Writing – review & editing.

Declaration of competing interest

The authors declare that they have no known competing financial interests or personal relationships that could have appeared to influence the work reported in this paper.

Data availability

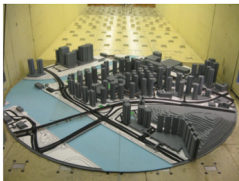
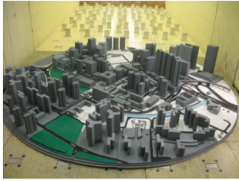
Data will be made available on request.

Acknowledgement

This research is supported by the General Research Fund (RGC Ref No. 14619121) from the Research Grants Council (RGC) of Hong Kong.

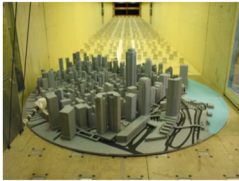
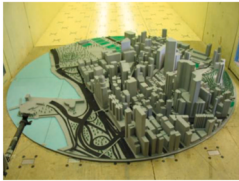
Appendix A. Wind Tunnel Models

Table 3
Reduced-scale urban models (1: 400) in the wind tunnel experiments [53,54].

Site	Urban model image	Site	Urban model image
Tsuen Wan, Kowloon		Sha Tin, New Territories	
Mong Kok, Kowloon		San Po Kong, Kowloon	

(continued on next page)

Table 3 (continued)

Site	Urban model image	Site	Urban model image
Tseung Kwan O, New Territories		Tsim Sha Tsui, Kowloon	
Sheung Wan, Hong Kong Island		Causeway Bay, Hong Kong Island	
Wong Chuk Hang, Hong Kong Island			

Appendix B. LiDAR Upper-air Wind Data

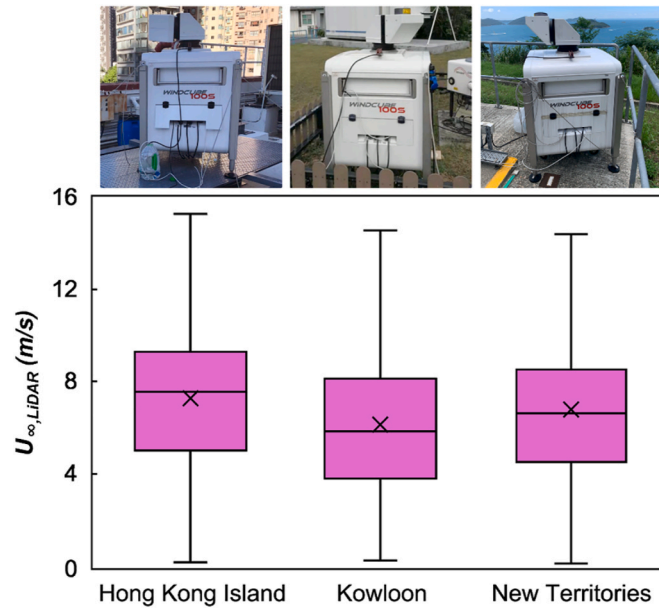


Fig. 16. Distributions of mean wind speed at 500 m above the ground ($U_{\infty, LiDAR}$) observed by wind LiDAR in Hong Kong Island, Kowloon, and New Territories in summers of 2020 and 2021.

References

[1] Intergovernmental Panel on Climate Change (IPCC), Summary for policymakers, in: Climate Change 2021: the Physical Science Basis. Contribution of Working Group I to the Sixth Assessment Report of the Intergovernmental Panel on Climate Change, Cambridge University Press, 2021.

[2] A.M. Rizwan, L.Y. Dennis, L. Chunho, A review on the generation, determination and mitigation of Urban Heat Island, J. Environ. Sci. 20 (1) (2008) 120–128.

[3] M. Krzyzanowski, B. Kuna-Dibbert, J. Schneider, Health Effects of Transport-Related Air Pollution, WHO Regional Office Europe, 2005.

[4] Hong Kong Observatory (HKO), Climatological database. 2022 [cited 2022 June 15]. <https://www.hko.gov.hk/en/cis/climat.htm>.

[5] E. Ng, Policies and technical guidelines for urban planning of high-density cities—air ventilation assessment (AVA) of Hong Kong, Build. Environ. 44 (7) (2009) 1478–1488.

- [6] Housing, Planning and Lands Bureau and Environment, Transport and Works Bureau, Technical Circular NO. 1/06: Air Ventilation Assessments, HPLB and ETWB, Hong Kong, 2006.
- [7] Planning Department (PlanD), Chapter 11 Urban Design Guidelines, Hong Kong Planning Standards and Guidelines, PlanD, Hong Kong, 2016.
- [8] Building Department (BD), Sustainable Building Design Guidelines (APP-152), BD, Hong Kong, 2011.
- [9] H.E. Landsberg, *The Urban Climate*, Academic press, 1981.
- [10] C. Grimmond, T.R. Oke, Aerodynamic properties of urban areas derived from analysis of surface form, *J. Appl. Meteorol. Climatol.* 38 (9) (1999) 1262–1292.
- [11] Y. He, C. Ren, H.W.L. Mak, C. Lin, Z. Wang, J.C.H. Fung, Y. Li, A.K.H. Lau, E. Ng, Investigations of high-density urban boundary layer under summer prevailing wind conditions with Doppler LiDAR: a case study in Hong Kong, *Urban Clim.* 38 (2021), 100884.
- [12] J.R. Garratt, The atmospheric boundary layer, *Earth Sci. Rev.* 37 (1–2) (1994) 89–134.
- [13] S.R. Hanna, J.C. Chang, Boundary-layer parameterizations for applied dispersion modeling over urban areas, *Boundary-Layer Meteorol.* 58 (3) (1992) 229–259.
- [14] M.R. Raupach, R.A. Antonia, S. Rajagopalan, *Rough-wall Turbulent Boundary Layers*, 1991.
- [15] J. Counihan, Wind tunnel determination of the roughness length as a function of the fetch and the roughness density of three-dimensional roughness elements, *Atmos. Environ.* 5 (8) (1971) 637–642.
- [16] J. Kondo, H. Yamazawa, Aerodynamic roughness over an inhomogeneous ground surface, *Boundary-Layer Meteorol.* 35 (4) (1986) 331–348.
- [17] J.E. Kutzbach, Investigations of the modification of wind profiles by artificially controlled surface roughness, *Stud. Three Dimen. Struct. Planet. Bound. Layer* (1961) 71–113.
- [18] M. Bottema, Urban roughness modelling in relation to pollutant dispersion, *Atmos. Environ.* 31 (18) (1997) 3059–3075.
- [19] R. Macdonald, R. Griffiths, D. Hall, An improved method for the estimation of surface roughness of obstacle arrays, *Atmos. Environ.* 32 (11) (1998) 1857–1864.
- [20] M. Raupach, Simplified expressions for vegetation roughness length and zero-plane displacement as functions of canopy height and area index, *Boundary-Layer Meteorol.* 71 (1) (1994) 211–216.
- [21] J. Wieringa, Updating the Davenport roughness classification, *J. Wind Eng. Ind. Aerod.* 41 (1–3) (1992) 357–368.
- [22] J. Wieringa, Representative roughness parameters for homogeneous terrain, *Boundary-Layer Meteorol.* 63 (4) (1993) 323–363.
- [23] A. Matzarakis, H. Mayer, Mapping of urban air paths for planning in Munich, *Wiss. Ber. Inst. Meteor. Klimaforsch. Univ. Karlsruhe* 16 (1992) 13–22.
- [24] T. Kubota, M. Miura, Y. Tominaga, A. Mochida, Wind tunnel tests on the relationship between building density and pedestrian-level wind velocity: development of guidelines for realizing acceptable wind environment in residential neighborhoods, *Build. Environ.* 43 (10) (2008) 1699–1708.
- [25] T. Gál, J. Unger, Detection of ventilation paths using high-resolution roughness parameter mapping in a large urban area, *Build. Environ.* 44 (1) (2009) 198–206.
- [26] M.S. Wong, J.E. Nichol, P.H. To, J. Wang, A simple method for designation of urban ventilation corridors and its application to urban heat island analysis, *Build. Environ.* 45 (8) (2010) 1880–1889.
- [27] E. Ng, C. Yuan, L. Chen, C. Ren, J.C. Fung, Improving the wind environment in high-density cities by understanding urban morphology and surface roughness: a study in Hong Kong, *Landscape Urban Plann.* 101 (1) (2011) 59–74.
- [28] A. Suder, M. Szymanowski, Determination of ventilation channels in urban area: a case study of Wrocław (Poland), *Pure Appl. Geophys.* 171 (6) (2014) 965–975.
- [29] C. Yuan, C. Ren, E. Ng, GIS-based surface roughness evaluation in the urban planning system to improve the wind environment—A study in Wuhan, China, *Urban Clim.* 10 (2014) 585–593.
- [30] P. Xie, J. Yang, H. Wang, Y. Liu, Y. Liu, A New method of simulating urban ventilation corridors using circuit theory, *Sustain. Cities Soc.* 59 (2020), 102162.
- [31] C.M. Hsieh, H.C. Huang, Mitigating urban heat islands: a method to identify potential wind corridor for cooling and ventilation, *Comput. Environ. Urban Syst.* 57 (2016) 130–143.
- [32] L. Tschritzis, M. Nikolopoulou, The effect of building height and façade area ratio on pedestrian wind comfort of London, *J. Wind Eng. Ind. Aerod.* 191 (2019) 63–75.
- [33] O. Palusci, P. Monti, C. Cecere, H. Montazeri, B. Blocken, Impact of Morphological Parameters on Urban Ventilation in Compact Cities: the Case of the Tuscolano-Don Bosco District in Rome, vol. 807, *Science of the Total Environment*, 2022, 150490.
- [34] J. Savins, Drag reduction characteristics of solutions of macromolecules in turbulent pipe flow, *Soc. Petrol. Eng. J.* 4 (3) (1964) 203–214.
- [35] C. Gromke, R. Buccolieri, S. Di Sabatino, B. Ruck, Dispersion study in a street canyon with tree planting by means of wind tunnel and numerical investigations—evaluation of CFD data with experimental data, *Atmos. Environ.* 42 (37) (2008) 8640–8650.
- [36] Planning Department (PlanD), Site Wind Availability Data, PlanD, 2019 [cited 2022 May 15]; Available from: https://www.pland.gov.hk/pland_en/info_serv/site_wind/index.html.
- [37] Architectural Institute of Japan (AIJ), AIJ Recommendations for Loads on Buildings, AIJ, Japan, 1996.
- [38] Building Department (BD), New Territories Exempted Houses, BD, 2018 [cited 2022 May 15]; Available from: https://www.bd.gov.hk/en/safety-inspection/ubw/UBW-in-new-territories-exempted-houses/index_ubw_nteh_intro.html.
- [39] ESRI, Euclidean allocation (spatial analyst) [cited 2022 May 15]; Available from: <https://pro.arcgis.com/en/pro-app/2.8/tool-reference/spatial-analyst/euclidean-allocation.htm>, 2022.
- [40] T.R. Oke, Street design and urban canopy layer climate, *Energy Build.* 11 (1–3) (1988) 103–113.
- [41] T. Li, F. Shilling, J. Thorne, F. Li, H. Schott, R. Boynton, A.M. Berry, Fragmentation of China's landscape by roads and urban areas, *Landscape Ecol.* 25 (6) (2010) 839–853.
- [42] S.A. Poessel, C.L. Burdett, E.E. Boydston, L.M. Lyren, R.S. Alonso, R.N. Fisher, K. R. Crooks, Roads influence movement and home ranges of a fragmentation-sensitive carnivore, the bobcat, in an urban landscape, *Biol. Conserv.* 180 (2014) 224–232.
- [43] X. Shen, Z. Gao, W. Ding, Y. Yu, An investigation on the effect of street morphology to ambient air quality using six real-world cases, *Atmos. Environ.* 164 (2017) 85–101.
- [44] Y. He, A. Tablada, N.H. Wong, Effects of non-uniform and orthogonal breezeway networks on pedestrian ventilation in Singapore's high-density urban environments, *Urban Clim.* 24 (2018) 460–484.
- [45] X. Guo, R. Buccolieri, Z. Gao, M. Zhang, T. Lyu, L. Rui, J. Shen, On the effects of urban-like intersections on ventilation and pollutant dispersion, in: *Building Simulation*, Springer, 2022.
- [46] X. Wang, K. McNamara, Effects of street orientation on dispersion at or near urban street intersections, *J. Wind Eng. Ind. Aerod.* 95 (9–11) (2007) 1526–1540.
- [47] M.F. Yassin, R. Kellnerova, Z. Jaour, Impact of street intersections on air quality in an urban environment, *Atmos. Environ.* 42 (20) (2008) 4948–4963.
- [48] Y. He, A. Tablada, N.H. Wong, A parametric study of angular road patterns on pedestrian ventilation in high-density urban areas, *Build. Environ.* 151 (2019) 251–267.
- [49] K.J. Amos, J. Peakall, P.W. Bradbury, M. Roberts, G. Keevil, S. Gupta, The influence of bend amplitude and planform morphology on flow and sedimentation in submarine channels, *Mar. Petrol. Geol.* 27 (7) (2010) 1431–1447.
- [50] A.M.F. da Silva, T. El-Tahawy, W.D. Tape, Variation of flow pattern with sinuosity in sine-generated meandering streams, *J. Hydraul. Eng.* 132 (10) (2006) 1003–1014.
- [51] L. Adolphe, A simplified model of urban morphology: application to an analysis of the environmental performance of cities, *Environ. Plann. Plann. Des.* 28 (2) (2001) 183–200.
- [52] B. Li, J. Liu, M. Li, Wind tunnel study on the morphological parameterization of building non-uniformity, *J. Wind Eng. Ind. Aerod.* 121 (2013) 60–69.
- [53] Planning Department (PlanD), Working Paper 2B: Wind Tunnel Benchmarking Studies – Batch I, Urban Climatic Map and Standards for Wind Environment – Feasibility Study, PlanD, Hong Kong, 2008.
- [54] Planning Department (PlanD), Working Paper 2C: Wind Tunnel Benchmarking Studies – Batch II, Urban Climatic Map and Standards for Wind Environment – Feasibility Study, PlanD, Hong Kong, 2010.
- [55] G. Falkovich, *Fluid Mechanics: A Short Course for Physicists*, Cambridge University Press, 2011.
- [56] J. Gandemer, A. Guyot, *Intégration du phénomène vent dans la conception du milieu bâti*, Ministère de la Qualité de la Vie, Paris, 1976.
- [57] R.X. Lee, N.H. Wong, A.Y.K. Tan, S.K. Jusuf, The study of variation in Gross Building Coverage Ratio on estate-level outdoor ventilation, in: *ICSDC 2011: Integrating Sustainability Practices in the Construction Industry*, 2012, pp. 255–264.
- [58] K. Ahmad, M. Khare, K. Chaudhry, Wind tunnel simulation studies on dispersion at urban street canyons and intersections—a review, *J. Wind Eng. Ind. Aerod.* 93 (9) (2005) 697–717.
- [59] X.-X. Li, C.H. Liu, D.Y. Leung, K.M. Lam, Recent progress in CFD modelling of wind field and pollutant transport in street canyons, *Atmos. Environ.* 40 (29) (2006) 5640–5658.
- [60] E.D. Lazarus, J.A. Constantine, Generic theory for channel sinuosity, *Proc. Natl. Acad. Sci. USA* 110 (21) (2013) 8447–8452.
- [61] B. Li, J. Liu, J. Gao, Surface wind pressure tests on buildings with various non-uniformity morphological parameters, *J. Wind Eng. Ind. Aerod.* 137 (2015) 14–24.
- [62] S.A. Zaki, A. Hagishima, J. Tanimoto, N. Ikegaya, Aerodynamic parameters of urban building arrays with random geometries, *Boundary-Layer Meteorol.* 138 (1) (2011) 99–120.
- [63] Y. He, C. Yuan, C. Ren, E. Ng, Urban ventilation assessment with improved vertical wind profile in high-density cities – comparisons between LiDAR and conventional methods, *J. Wind Eng. Ind. Aerod.* 228 (2022) 105116.
- [64] Y. He, C. Yuan, C. Ren, W. Wang, Y. Shi, E. Ng, Urban ventilation assessment with improved vertical wind profile in high-density cities – investigations in nighttime extreme hot weather events, *Build. Environ.* 216 (2022), 109018.
- [65] V. Cheng, E. Ng, Thermal comfort in urban open spaces for Hong Kong, *Architect. Sci. Rev.* 49 (3) (2006) 236–242.
- [66] C. Yuan, E. Ng, Building porosity for better urban ventilation in high-density cities—A computational parametric study, *Build. Environ.* 50 (2012) 176–189.
- [67] Y. He, A. Tablada, J. Deng, Y. Shi, N.H. Wong, E. Ng, Linking of Pedestrian Spaces to Optimize Outdoor Air Ventilation and Quality in Tropical High-Density Urban Areas, *Urban Climate*, 2022.
- [68] Y. Shi, K.K.L. Lau, E. Ng, Developing street-level PM_{2.5} and PM₁₀ land use regression models in high-density Hong Kong with urban morphological factors, *Environ. Sci. Technol.* 50 (15) (2016) 8178–8187.